Glycobiology, 2016, vol. 26, no. 7, 701–709
doi: 10.1093/glycob/cww011
Advance Access Publication Date: 5 February 2016
Original Article

OXFORD

Chemical Biology

N-Arylacyl *O*-sulfonated aminoglycosides as novel inhibitors of human neutrophil elastase, cathepsin G and proteinase 3

Ioana Craciun, Amanda M Fenner, and Robert J Kerns[1]

Division of Medicinal and Natural Products Chemistry, Department of Pharmaceutical Sciences and Experimental Pharmaceutics, University of Iowa College of Pharmacy, Iowa City, IA 52242, USA

[1]To whom correspondence should be addressed: Tel: +1-319-335-8800; Fax: +1-319-335-8766; e-mail: robert-kerns@uiowa.edu

Received 4 August 2015; Revised 19 January 2016; Accepted 23 January 2016

Abstract

The balance between neutrophil serine proteases (NSPs) and protease inhibitors (PIs) in the lung is a critical determinant for a number of chronic inflammatory lung diseases such as chronic obstructive pulmonary disease, cystic fibrosis and acute lung injury. During activation at inflammatory sites, excessive release of NSPs such as human neutrophil elastase (HNE), proteinase 3 (Pr3) and cathepsin G (CatG), leads to destruction of the lung matrix and continued propagation of acute inflammation. Under normal conditions, PIs counteract these effects by inactivating NSPs; however, in chronic inflammatory lung diseases, there are insufficient amounts of PIs to mitigate damage. Therapeutic strategies are needed to modulate excessive NSP activity for the clinical management of chronic inflammatory lung diseases. In the study reported here, a panel of *N*-arylacyl *O*-sulfonated aminoglycosides was screened to identify inhibitors of the NSPs. Dose-dependent inhibitors for each individual serine protease were identified. Select compounds were found to inhibit multiple NSPs, including one lead structure that is shown to inhibit all three NSPs. Two lead compounds identified during the screen for each individual NSP were further characterized as partial mixed inhibitors of CatG. Concentration-dependent inhibition of protease-mediated detachment of lung epithelial cells is demonstrated.

Key words: glycosaminoglycans, heparin mimics, inflammatory lung disease, neutrophil serine proteases, protease inhibitors

Introduction

In chronic inflammatory lung diseases such as cystic fibrosis, bronchiectasis, acute lung injury and chronic obstructive pulmonary disease, inflammation becomes excessive and there is an abnormal increase of inflammatory cells present in the airways, especially polymorphonuclear neutrophils (PMNs) (Owen 2008). PMNs are essential for protection against invading pathogens and are the primary mediators of inflammatory response (Hahn et al. 2011). During inflammation PMNs migrate from the blood to the injured tissue, where they release three neutrophil serine proteases (NSPs) stored in their primary granules: human neutrophil elastase (HNE), proteinase 3 (Pr3) and cathepsin G (CatG) (Owen et al. 1994; Owen and Campbell 1999). NSPs play a critical role in the innate immune system, however, if unregulated their action can be detrimental and results in degradation of the host tissue (Pham 2006; Kessenbrock et al. 2011; Guyot et al. 2014). Endogenous protease inhibitors (PIs) protect the host from these potentially damaging effects by regulating the activity of NSPs. However, in inflammatory lung diseases, there is an imbalance between NSP secretion and PIs available to modulate NSP activity (Turino 2002). This imbalance has been proven to lead to excessive, protease propagated, inflammation and contributes to the pathogenesis of inflammatory lung diseases (Lucas et al. 2013).

A great deal of effort has been invested in the development of synthetic (Ohbayashi 2002; Lucas et al. 2013) as well as natural (Barnes 2008; Zani et al. 2009, 2011) NSP inhibitors to restore the protease–antiprotease imbalance in inflammatory lung diseases. Current synthetic, small molecule NSP inhibitors have had little success due to the fact that they are generally designed to target one NSP, mainly

HNE, with only a few reports of inhibitors designed to target two of the three proteases (Hwang et al. 2015). Endogenous or recombinant NSP inhibitors such as elafin and secretory leukocyte protease inhibitor (SLPI) are also unable to simultaneously inhibit all three NSPs; they are also susceptible to proteolysis and producing large quantities of a protein for therapeutic use is not cost effective when compared with small molecule agents (Barnes 2008; Korkmaz et al. 2010).

Under normal inflammatory response, the protease–antiprotease balance is maintained through the secretion of endogenous PIs and additional endogenous inhibitors such as heparan sulfate (Spencer et al. 2006). Heparan sulfate is a cell-surface glycosaminoglycan (GAG) comprised of repeating disaccharide units with regions of high anionic content, which selectively and/or nonselectively binds to many proteins. During inflammation heparan sulfate is cleaved from the cell surface by HNE resulting in a feedback mechanism that may limit elastase activity (Spencer et al. 2006). Heparin, a highly sulfated GAG that is structurally similar to heparan sulfate, as well as various heparin derivatives have been explored for their therapeutic potential as inhaled therapeutics for the treatment of chronic inflammatory lung diseases (Rao et al. 1990; Spencer et al. 2006; Qian et al. 2014). Heparin is a potent inhibitor of HNE, and moderately inhibits Pr3 and CatG. However, heparin as well as low-molecular-weight heparins inhibit the proteolytic activity of NSPs in a hyperbolic manner (Sissi et al. 2006; Fleddermann et al. 2012); therefore, dosing above or below the optimal inhibitory concentrations results in activation or retention of NSP activity. Another fundamental problem with using heparin as a potential treatment for inflammatory lung diseases is that polysulfated polysaccharides nonselectively bind many GAG-binding proteins resulting in undesirable off-target effects. For example, it is known that heparin not only binds and inhibits NSPs it also binds the endogenous PIs α-1 proteinase inhibitor, SLPI and elafin (Frommherz et al. 1991; Spencer et al. 2006; Gupta and Gowda 2008). More recently, Desai and coworkers have been studying sulfated low-molecular-weight lignins and other sulfated polymers for serine protease inhibition and other activities toward treating inflammatory lung diseases (Henry et al. 2012; Saluja et al. 2013, 2014).

We previously demonstrated that the high degree of nonspecific protein binding seen with heparin can be mitigated by synthesizing heparin derivatives substituted with aromatic residues in place of the *N*-sulfo or carboxylate groups (Fernandez et al. 2006; Huang and Kerns 2006; Huang et al. 2007). Incorporating non-anionic aryl moieties into heparin replaces nonspecific charge–charge binding contacts between heparin and target protein with more sterically hindered and selective cation-π binding interactions (Fernandez et al. 2006; Huang and Kerns 2006; Huang et al. 2007). These chemically modified heparin derivatives selectively bind certain heparin-binding proteins and also, due to the reduced charge–charge interactions have lower nonspecific binding. Using this approach, we recently synthesized and structurally characterized members of a panel of *N*-arylacyl *O*-sulfonated aminoglycosides (Figure 1; Supplementary data) as low-molecular-weight structural mimics of heparin (Fenner and Kerns 2011; Fenner et al. 2013). However, they are smaller, lower

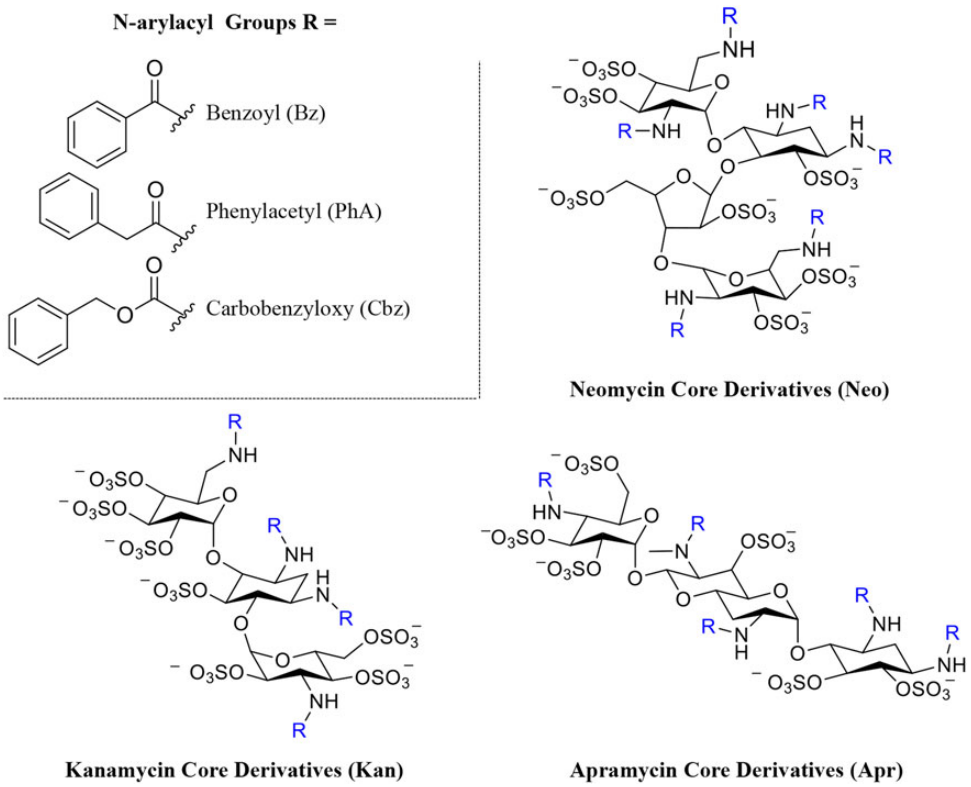

Fig. 1. Structures and degree of sulfation (DS) of *N*-arylacyl *O*-sulfonated aminoglycosides used in this study. The three aminoglycoside neomycin, kanamycin and apramycin are N-substituted with three different arylacyl groups and per-O-sulfonated, affording the panel of nine derivatives: *N*-carbobenzyloxy *O*-sulfonated neomycin (**NeoCbz**, DS = 7), *N*-phenylacetyl O-sulfonated neomycin (**NeoPhA**, DS = 6.8), *N*-benzoyl *O*-sulfonated neomycin (**NeoBz**, DS = 7), *N*-carbobenzyloxy *O*-sulfonated kanamycin (**KanCbz**, DS = 6), *N*-phenylacetyl *O*-sulfonated kanamycin (**KanPhA**, DS = 5.8), *N*-benzoyl *O*-sulfonated kanamycin (**KanBz**, DS = 5.1), *N*-carbobenzyloxy *O*-sulfonated apramycin (**AprCbz**, DS = 6), *N*-phenylacetyl *O*-sulfonated apramycin (**AprPhA**, DS = 6), *N*-benzoyl *O*-sulfonated apramycin (**AprBz**, DS = 6). Complete synthesis and characterization of panel of compounds is described in Supplementary data. This figure is available in black and white in print and in color at *Glycobiology* online.

charged, tri- and tetra- saccharides that are more selective than heparin in binding various heparin-binding proteins.

In the present study, we screened our panel of *N*-arylacyl *O*-sulfonated aminoglycosides for inhibition of NSPs in order to identify novel, small molecule lead structures that would inhibit all three of the NSPs. As reported here, we not only identified dose-dependent selective inhibitors of the individual serine proteases but also an inhibitor of all three NSPs. Furthermore, these compounds do not exhibit the hyperbolic inhibition profile seen with heparin and other polysulfated polysaccharides. Using two lead compounds identified during the screen for each individual NSP, we characterized the type of inhibition these lead compounds have with respect to the serine proteases, as well as demonstrate that inhibition of the proteases in enzyme-based assays is translatable to blocking protease-mediated detachment of lung epithelial cells.

Results

Inhibition of NSPs by *N*-arylacyl *O*-sulfonated aminoglycosides

Each member of our panel of *N*-arylacyl *O*-sulfonated aminoglycosides was first screened for inhibition of each NSP using a peptide cleavage assay. The protease inhibition profile for each derivative, grouped based on common aminoglycoside core structure, with HNE (Figure 2A–C), CatG (Figure 2D–F) and Pr3 (Figure 2G–I) is shown, and the IC_{50} values for each compound with each NSP are summarized in Table I. None of the compounds achieved complete inhibition of HNE (Figure 2A–C). **NeoCbz**, depicted by closed circle (Figure 2A), was the most potent HNE inhibitor (IC_{50} 8.13 μM). As a general trend, the carbobenzyloxy derivatives were the most potent inhibitors of HNE, the phenylacetyl derivatives inhibited HNE only at high concentrations with IC_{50} values in the 250 μM range, and the benzoyl substituted derivatives did not achieve 50% inhibition of HNE, regardless of the aminoglycoside core (Figure 2A–C). It is apparent that inhibition of HNE is strongly dependent on the *N*-aryl functional group and to a lesser extent on the aminoglycoside core. For the carbobenzyloxy derivatives, the phenyl moiety is positioned further out from the aminoglycoside core, and is thus likely able to not only reach and occupy a deeper binding pocket but also make multiple binding contacts with cationic residues on the surface of HNE. As the distance between the phenyl moiety and the aminoglycoside core is decreased the compounds lose their ability to bind and inhibit the enzyme, as was observed with the benzoyl derivatives.

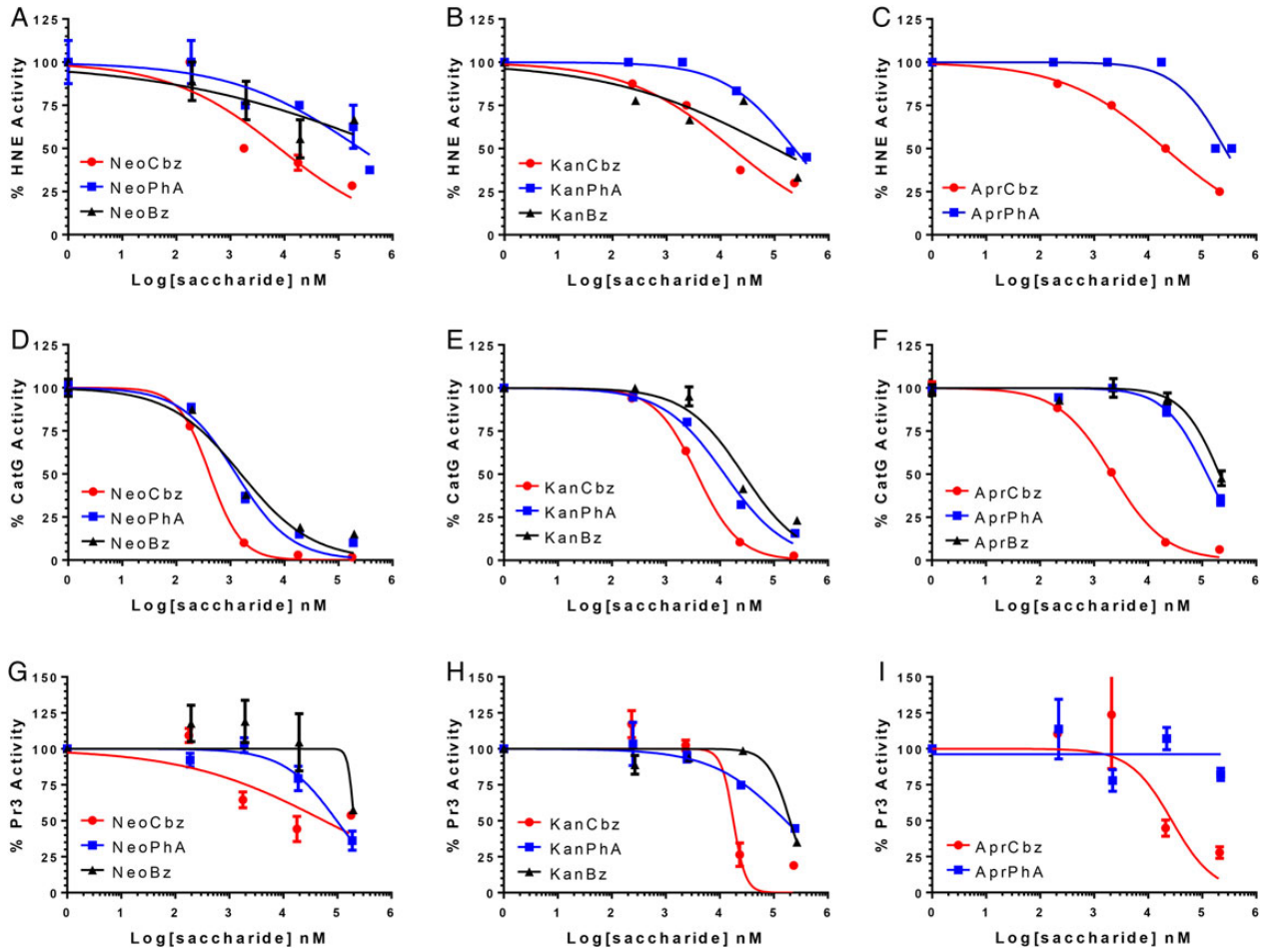

Fig. 2. NSP inhibition by *N*-arylacyl *O*-sulfonated aminoglycosides. (**A**–**C**) Dose-dependent inhibition of HNE by neomycin, kanamycin and apramycin derivatives, respectively; (**D**–**F**) dose-dependent inhibition of CatG by neomycin, kanamycin and apramycin derivatives, respectively; (**G**–**I**) dose-dependent inhibition of Pr3 by neomycin, kanamycin and apramycin derivatives, respectively. Absorbance of *p*-nitroaniline released from a protease specific chromogenic substrate was measured at 405 nm and normalized to enzyme only control. Nonlinear regression curve fitting was performed to obtain IC_{50} values summarized in Table I. Data are presented as mean ± SE ($n = 3$). This figure is available in black and white in print and in color at *Glycobiology* online.

All compounds inhibited CatG to various degrees yielding IC_{50} values ranging from 0.42 μM for **NeoCbz** to 219 μM for **AprBz** (Figure 2D–F). The concentration-dependent inhibitory profiles showed that the neomycin core derivatives (Figure 2D) were the most potent inhibitors of CatG, followed by the kanamycin core derivatives (Figure 2E) with slightly reduced potency and apramycin derivatives with the lowest overall potency as a group (Figure 2F). When comparing the *N*-aryl functional groups, the carbobenzyloxy derivatives, were the most potent inhibitors while the benzoyl derivatives were the weakest. These results suggest that a more flexible core and *N*-aryl derivative is generally favored for CatG inhibition.

Pr3 activity was moderately inhibited by **KanCbz** (Figure 2H) and **AprCbz** (Figure 2I). Interestingly **NeoCbz**, the most potent inhibitor of HNE and CatG, did not achieve 50% inhibition of Pr3 (Figure 2G). Similarly to the results obtained with HNE, the phenylacetyl derivatives were weak inhibitors of Pr3, while the benzoyl derivatives showed an inhibitory effect only at high concentrations and did not achieve 50% inhibition. All of the compounds were dose-dependent, non-hyperbolic inhibitors of the three NSPs.

The inhibition of CatG, HNE and Pr3 by our panel of *N*-arylacyl *O*-sulfonated aminoglycosides revealed *O*-sulfonated *N*-carbobenzyloxy Kanamycin as a novel inhibitor of all three NSPs, and *O*-sulfonated *N*-carbobenzyloxy Neomycin as a potent inhibitor of HNE and CatG. These two compounds were thus subsequently used to perform initial velocity studies to determine their mode of enzyme inhibition.

Table I. Half-maximal inhibitory concentration of *N*-arylacyl *O*-sulfonated aminoglycosides for inhibition of each NSP

Compound	Human neutrophil elastase[a], IC_{50} (μM)	Cathepsin G[b], IC_{50} (μM)	Proteinase 3[a], IC_{50} (μM)
NeoCbz	8.13 ± 3.49	0.42 ± 0.03	>300
NeoPhA	>300	1.29 ± 0.21	97.72 ± 22.75
NeoBz	>300	1.55 ± 0.36	>300
KanCbz	16.60 ± 7.55	3.72 ± 0.17	16.98 ± 5.18*
KanPhA	229.09 ± 58.99	12.3 ± 1.42	165.96 ± 58.75
KanBz	>300	26.92 ± 5.63	>300
AprCbz	20.42 ± 11.45	2.14 ± 0.2	26.92 ± 18.52
AprPhA	263.03 ± 30.37	123.03 ± 11.35	NI
AprBz	NI	208.93 ± 24.68	ND

NI, no inhibition; ND, not determined.

IC_{50} values derived from nonlinear regression curve fitting to log(inhibitor) vs. normalized response. Data are shown as mean ± SE ($n = 3$ or $^*n = 2$).

[a]Substrates: *N*-methoxysuccinyl-Ala-Ala-Pro-Val-*p*-nitroanilide.

[b]*N*-succinyl-Ala-Ala-Pro-Phe-*p*-nitroanilide.

Initial velocity studies with CatG and two lead compounds

From the analysis of each test compound's ability to inhibit each NSP, two compounds were chosen for further studies to determine their mechanism of inhibition. **NeoCbz** was chosen for its potent inhibition of HNE and CatG. **KanCbz** was selected for its ability to inhibit each of the three NSPs. The mechanism of protease inhibition was determined using CatG as the representative NSP. HNE, Pr3 and CatG are homologous cationic proteases, and we anticipate that each inhibitor will likely have the same general mechanism of inhibition for each protease. CatG inhibition was measured at four substrate concentrations (0.315 – 2 mM) in the absence or presence of inhibitors at various concentrations (0.5[IC_{50}] to 4[IC_{50}]). The data were fit using Michaelis–Menten kinetics and Lineweaver–Burk plots were prepared. From the Lineweaver–Burk plots, as inhibitor concentration is increased there is a decrease in V_{max} and an increase in K_m, thus indicating that both **KanCbz** (Figure 3A) and **NeoCbz** (Figure 3B) are partial mixed inhibitors of CatG with respect to the substrate.

Inhibition of NSP-mediated cell detachment

NSPs cleave cell-surface adhesion molecules such as intercellular adhesion molecule 1 and epithelial (E)-cadherin thus terminating cell–cell or cell–extracellular matrix interactions and causing degradation of the extracellular lung matrix in inflammatory lung diseases (Pham 2006). In order to gain an initial assessment of the potential for *N*-arylacyl *O*-sulfonated aminoglycosides to block the cleavage of cell-surface adhesion molecules and protect lung epithelial cells from

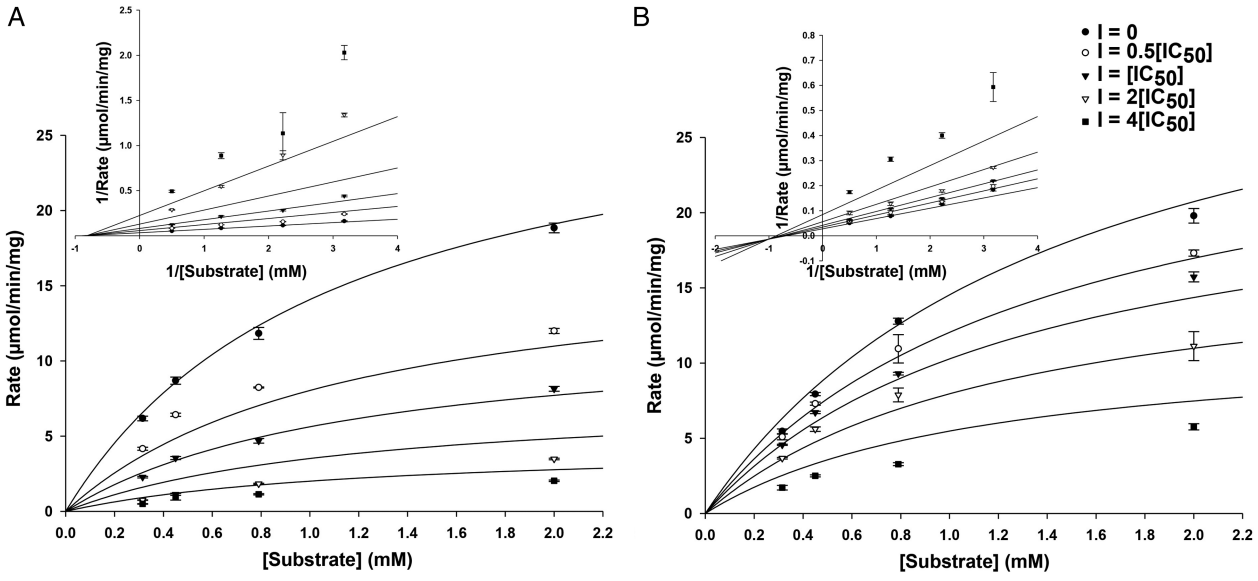

Fig. 3. Mode of CatG inhibition. Michaelis–Menten plot and double reciprocal Lineweaver-Burk plot (inset) of (**A**) **KanCbz** and (**B**) **NeoCbz** inhibition of CatG. The concentration of CatG chromogenic substrate was varied at four different inhibitor concentrations (0, 0.5[IC_{50}], [IC_{50}], 2[IC_{50}] and 4[IC_{50}]). Both compounds were partial mixed inhibitors of CatG.

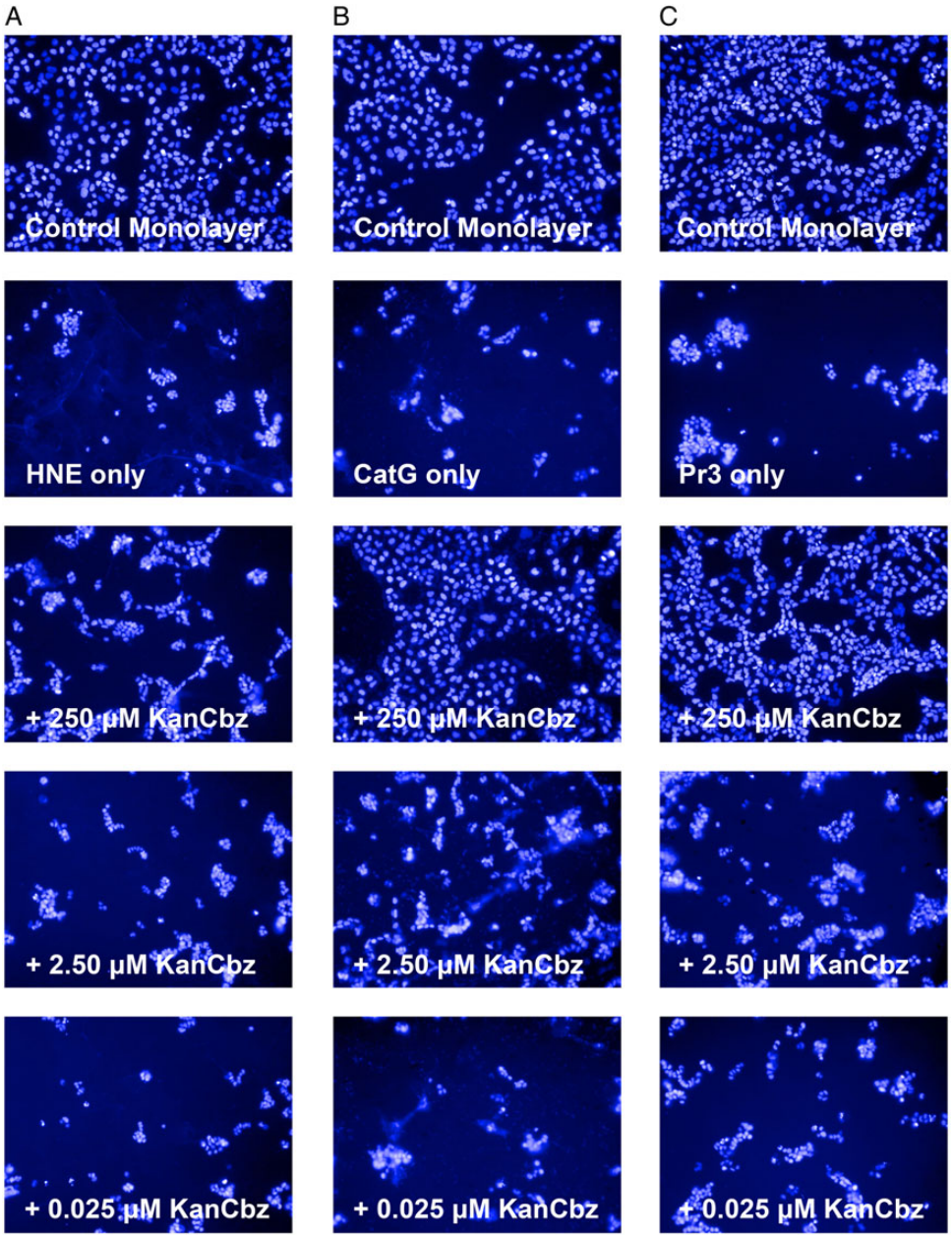

Fig. 4. Protection against protease-mediated cell detachment. A549 lung epithelial cells were exposed to (**A**) HNE (50 nM), (**B**) CatG (250 nM) or (**C**) Pr3 (50 nM) in the presence or absence of decreasing concentrations of **KanCbz**. The NSPs were pre-incubated with **KanCbz** (250, 2.50 and 0.025 μM) for 30 min on ice before addition to confluent A549 cells. After 24 h lung epithelial cell nuclei were stained with Hoechst 33342 and cells were imaged using Operetta High Content Imaging System. Only one representative field for each experiment is shown for clarity. At 250 μM **KanCbz** inhibits HNE-, CatG- and Pr3-induced cell detachment. At lower concentrations, this protection is lost and protease-mediated cell detachment is once again observed. This figure is available in black and white in print and in color at *Glycobiology* online.

proteolytic cell detachment induced by NSPs, we exposed cells to HNE, CatG and Pr3 in the presence and absence of decreasing concentrations of **KanCbz**, and imaged cells using the Operetta High Content Imaging System. When uninhibited, NSPs cause morphological changes to cells as well as detachment of cells. For this set of experiments, each NSP was incubated for 30 min with various concentrations of **KanCbz** before addition to a monolayer of A549 lung epithelial cells (Figure 4). Treatment of the cells with NSP-only control caused cell detachment and loss of the monolayer was observed. At the highest concentration of **KanCbz** used, complete protection against protease-induced cell detachment was observed for CatG (Figure 4B), and to a lesser extent with Pr3 (Figure 4C), while the least protection was observed in the presence of HNE (Figure 4A).

A549 lung epithelial cells were then incubated with each member of our panel of *N*-arylacyl *O*-sulfonated aminoglycosides in the presence of each NSPs and the remaining adherent cells were counted using the Harmony Analysis Software. **KanCbz** (Figure 5A–C) and **NeoCbz** (Figure 5D–F) were the only two compounds that showed a significant protection, at the highest concentration, against all three NSPs. Both compounds showed the least protection against HNE,

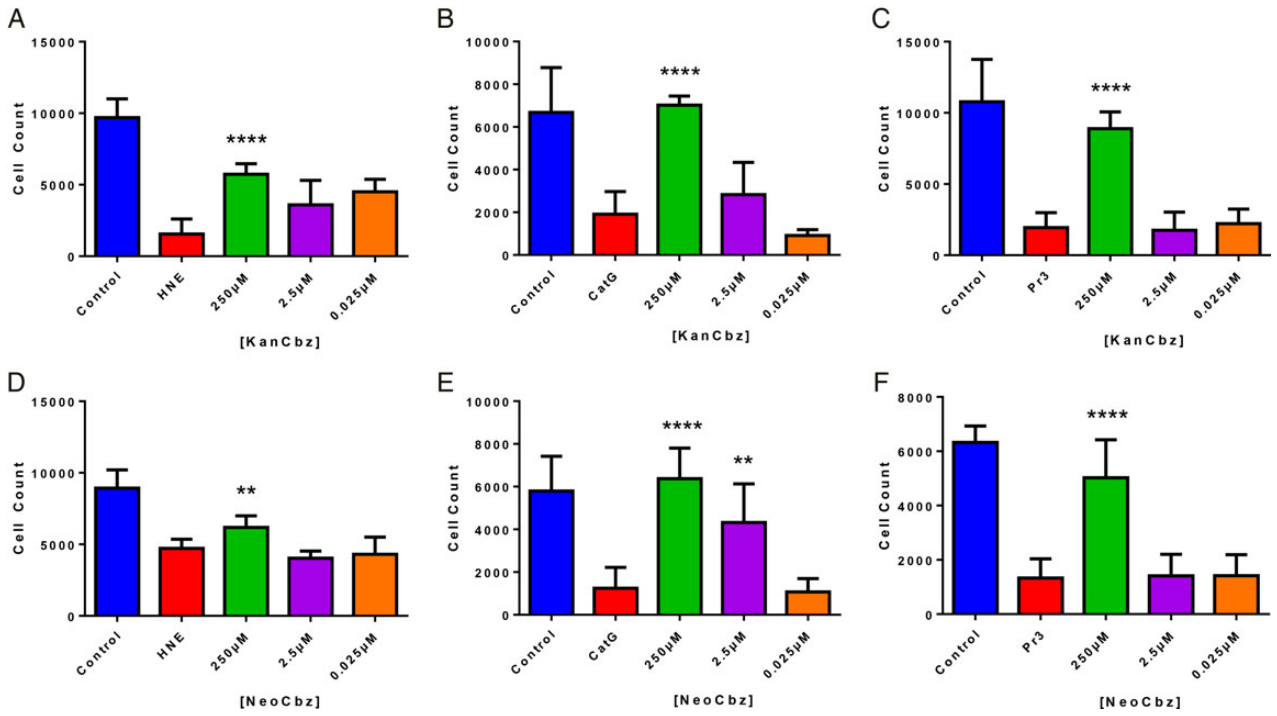

Fig. 5. Quantification of NSP-mediated cell detachment in the presence of two lead compounds. A549 lung epithelial cells were exposed to each NSP (50 nM HNE, 250 nM CatG or 50 nM Pr3) in the presence of decreasing concentrations of **KanCbz** (**A–C**) or **NeoCbz** (**D–F**). After 24 h lung epithelial cell nuclei were stained with Hoechst 33342 and cells were imaged and counted using an Operetta High Content Imaging System and Harmony Analysis Software, respectively. At the highest concentration, both **KanCbz** and **NeoCbz** protected cells against protease-mediated cell detachment. Data are presented as mean + SE, $^{**}P < 0.01$, $^{***}P < 0.001$ $^{****}P < 0.0001$ when compared with protease-treated cells ($n = 3$ from three experiments each done in triplicate). This figure is available in black and white in print and in color at *Glycobiology* online.

while almost completely inhibiting CatG- and Pr3-induced cell detachment at the highest concentration tested. At low concentrations, these protective effects are lost and protease-mediated cell detachment is once again observed. The complete quantification of concentration-dependent inhibition of HNE, CatG and Pr3 mediated cell detachment by each member of our panel of compounds is shown in Supplementary data, S1–S3.

Discussion

Structure–activity relationships from screening *N*-arylacyl *O*-sulfonated aminoglycosides

In general, the *N*-arylacyl *O*-sulfonated derivatives of neomycin and kanamycin were more potent inhibitors of the three NSPs when compared with the corresponding apramycin derivatives. These results indicate that a flexible core structure allows for more favorable binding to the proteases and inhibition of their proteolytic activity. Neomycin core derivatives are generally more flexible. This increased flexibility is partly a result of having four glycosidic or glycoside-like bonds in the neomycin structure. Kanamycin and apramycin derivatives have only two glycosidic or glycoside-like bonds; however, apramycin derivatives also possess a centered fused-ring system making them more rigid. The apramycin derivatives had consistently higher IC_{50} values and lower protease inhibition activity. It is expected that the binding sites for the *N*-arylacyl *O*-sulfonated aminoglycosides are most likely large and shallow, with pockets available for the *N*-aryl groups to potentially afford hydrophobic binding contacts. Thus, a flexible core accommodates structural changes for optimal binding to one or multiple proteases. The length of the aminoglycoside cores also appears to play a role in the potency of the compounds. Neomycin is a tetramer oligosaccharide and the **NeoCbz** derivative was the most potent inhibitor screened. Although the smaller **KanCbz** derivative, possessing a tri-saccharide core, had lower optimal inhibition with any single NSP, it was overall the more potent inhibitor of all three NSPs, making it a novel non-peptide-based small inhibitor of all three serine proteases.

The benzoyl substituted derivatives for each aminoglycoside core structure were either weak or did not inhibit the NSPs, suggesting that distance between the aryl sidechain functional group and the aminoglycoside core is necessary for making binding contacts on the surface of the NSPs. As this length is increased from the benzoyl to phenylacetyl to carbobenzyloxy derivatives, there is a consistent decrease in IC_{50} values. This effect was observed in the case of all three NSPs. Interestingly, members of our panel of *N*-arylacyl *O*-sulfonated aminoglycosides preferentially bind and completely inhibit CatG. Complete inhibition of HNE and Pr3 was not observed for any of the compounds tested, however, even moderate inhibition of all three serine proteases is most likely sufficient to modulate their activity and restore the protease–antiprotease imbalance and attenuate the inflammatory response. NSPs play an important role in protecting the host against invading pathogens and complete inhibition of these proteases with a potent compound could leave the patient vulnerable to opportunistic lung infections.

Kancbz and **NeoCbz** lead compounds are partial mixed inhibitors of CatG

HNE, CatG and Pr3 are sequentially homologous serine proteases belonging to the chymotrypsin family (Korkmaz et al. 2010). HNE and Pr3 have 56% sequence identity and 35% sequence identity with

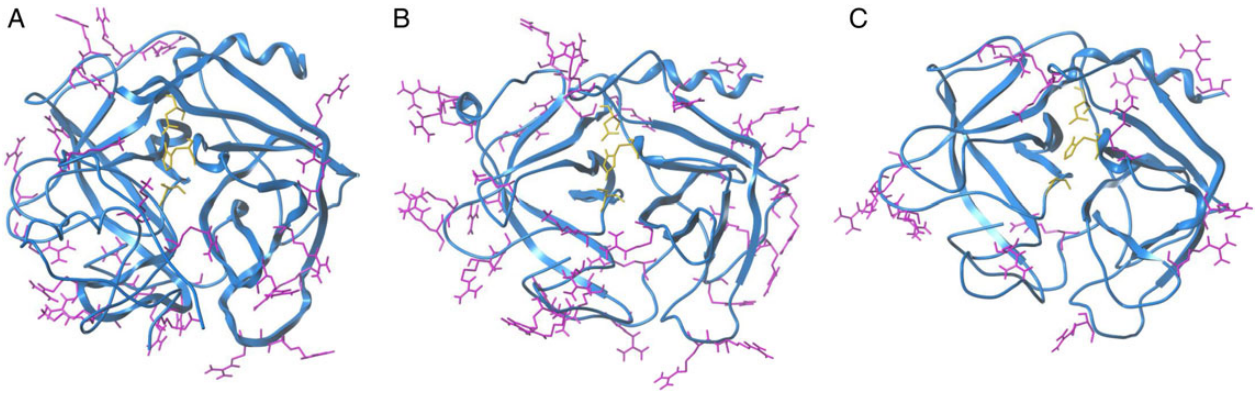

Fig. 6. Comparison of crystal structures of the three NSPs. Ribbon representation of (**A**) HNE (PDB: 1PPF) (**B**) CatG (PDB: 1CGH) and (**C**) Pr3 (PDB: 1FUJ). Arginine and lysine side chains are shown on the surface of the structures and side chains of the catalytic triad residues (His57, Asp102 and Ser195) in the center of each structure. This figure is available in black and white in print and in color at *Glycobiology* online.

CatG (Hajjar et al. 2010). The three proteases differ greatly in the surface distribution of the cationic amino acids (Figure 6). CatG is the most basic (p*I* of ~12) of the serine proteases followed by HNE and Pr3 (p*I* of ~10.5 and 9.5, respectively) which is the least basic of the three (Korkmaz et al. 2008). Evaluating the charge distribution as well as the p*I* values for each protease, it is not surprising that the compounds presented in this study preferentially inhibit CatG, and have a decreased potency towards Pr3. CatG also has a cluster of positively charged residues near the active site. These clusters of positively charged amino acids likely serve as binding sites for our panel of compounds.

We demonstrated that **KanCbz** and **NeoCbz** were partial mixed inhibitors of CatG, having both competitive and uncompetitive modes of enzyme inhibition, which leads us to believe that our compounds bind the serine proteases either at clusters of basic residues close to the catalytic site and/or further away from the active site on the surface of the protease, whether or not substrate is bound, and act as allosteric modulators of protease activity. These results also explain why complete inhibition of HNE and Pr3 was not observed for many of the compounds tested, while complete or near complete inhibition of CatG was observed for most compounds; partial mixed inhibitors reduce the catalytic activity of the enzyme-substrate-inhibitor complex without completely inhibiting its function. For example, docking studies (not shown) suggest the compounds here can bind in different poses, and with different affinities, to the clusters of positively charged residues near the protease active sites, thus each individual compound can impede substrate binding and reduce protease activity to a different level of maximum inhibition. These results are also consistent with the varied levels of fractional inhibition of serine proteases observed for sulfated low-molecular-weight lignins (Henry et al. 2012).

It is notable that synthetic PIs that do not directly compete with substrate for active site binding is favorable for modulating activity of lung proteases because the lung is saturated with protease substrates, which causes a loss of *in vivo* efficacy for competitive inhibitors (Drag and Salvesen 2010). Indeed, small molecule active site inhibitors have been optimized to be potent PIs having *in vitro* IC_{50} values in the mid nanomolar range; however, such compounds typically target only one of the three proteases, and require higher doses *in vivo* (Ohbayashi 2002). Therapeutic reduction of protease activity in the lung will hopefully restore the protease–PI balance without leaving patients susceptible to infections that trigger exacerbations (Sethi 2010). Use of endogenous or recombinant NSP inhibitors such as elafin and SLPI has also been unsuccessful to date because they do not simultaneously inhibit all three NSPs and they are susceptible to proteolysis. Larger nonpeptidic sulfated macromolecules that target multiple mechanisms of inflammation, even though they are less potent *in vitro*, have been shown to retain their activity in vivo (Saluja et al. 2013), and to attenuate elastase- and cigarette smoke extract-induced emphysema in rats (Saluja et al. 2014). Furthermore, proinflammatory mediators such as Interleukin-8 have been shown to bind heparan sulfate as well as other GAGs leading to activation and recruitment of neutrophils to the site of inflammation (Webb et al. 1993; Dias-Baruffi et al. 1998). We anticipate that compounds screened in this study, and future derivatives optimized for more potent inhibition of all three proteases, will maintain their activity when dosed directly to the lung, without a significant increase in IC_{50} by allosterically modulating the function of the three NSPs, as well as potentially interacting with key proinflammatory mediators to block their ability to recruit neutrophils.

KanCbz and **NeoCbz** protection of lung epithelial cells from NSP-mediated cell detachment

Because select *N*-arylacyl *O*-sulfonated aminoglycosides inhibited the proteolytic cleavage of chromogenic peptide substrates, we examined if this inhibition would translate to functional inhibition of the protease-mediated cleavage of cell-surface adhesion molecules in cell culture. To test for cell-based activity, we evaluated the ability of each member of our panel of *N*-arylacyl *O*-sulfonated aminoglycosides to inhibit HNE-, CatG- and Pr3-induced detachment of lung epithelial cells. HNE, as well as CatG and Pr3 are known to cleave components of the extracellular matrix thus causing degradation of the lung matrix (Pham 2006; Lu et al. 2011). A549 lung epithelial cells form a uniform monolayer covering the bottom of control wells on the surface of an uncoated 96-well plate. When each NSP is added, detachment of cells can be observed. Also the cell morphology drastically changes, cells are rounded and a majority of them have lost their membrane integrity. At high concentrations **KanCbz** and **NeoCbz** significantly protected the cells from detachment induced by HNE, CatG as well as Pr3, and the cell morphology resembled that of the control cells. At low concentrations of inhibitor, this protective effect was no longer observed and once again the monolayer was lost, cells were detached and their membrane integrity suffered similarly to that of protease only treated wells.

In conclusion, **KanCbz** was identified as a novel inhibitor of HNE, CatG and Pr3, and **NeoCbz** was shown to be a potent dual inhibitor of HNE and CatG. **KanCbz** and **NeoCbz** are partial mixed inhibitors of CatG and can bind and inhibit the protease even if substrate is bound. **KanCbz** and **NeoCbz** also protected lung epithelial cells from NSP-mediated proteolytic detachment. Several of the compounds screened had moderate activity towards all three NSPs, thus allowing us to construct initial structure–activity relationship models. This proof-of-concept study demonstrates that *N*-arylacyl *O*-sulfonated aminoglycosides, and likely other similar *N*-arylacyl *O*-sulfonated saccharide-based scaffolds, can be exploited as a promising new type of lead structure for further optimization toward the development of novel, multi-target NSP inhibitors that could be formulated for direct delivery to the lung by inhalation. Using the compounds described in this work as new molecular probes, ongoing studies to determine the effects of *N*-arylacyl *O*-sulfonated aminoglycosides on endogenous PIs and on GAG-binding mediators of inflammation are underway. This work will characterize the NSP inhibitory profile and other interactions in the lung that could potentially contribute to effectively blocking protease damage, decreasing inflammation and restoring the protease-anti protease balance. **KanCbz** is currently being evaluated in mouse models of toxicant-induced lung damage, by direct administration to the lung, to further validate this chemotype of molecule for further structural and functional optimization toward the development of an inhaled therapeutic for attenuating protease-mediated inflammatory lung diseases.

Methods

Enzymes and materials

Human neutrophil elastase (HNE, EC 3.4.21.37) was purchased from Calbiochem (EMD Chemicals, San Diego, CA), human proteinase 3 (Pr3, EC 3.4.21.76) and human Cathepsin G (CatG, EC 3.4.21.20) were purchased from Cell Sciences (Canton, MA). HNE- and Pr3-specific substrate *N*-methoxysuccinyl-Ala-Ala-Pro-Val-*p*-nitroanilide and CatG-specific substrate *N*-succinyl-Ala-Ala-Pro-Phe-*p*-nitroanilide were purchased from Sigma-Aldrich (St. Louis, MO).

Enzyme inhibition assay

Inhibition of HNE, Pr3 and CatG by *N*-arylacyl *O*-sulfonated aminoglycosides was measured using a chromogenic substrate hydrolysis assay (Fleddermann et al. 2012). Compounds at various concentrations ranging from 0.001 to 2 mg/mL were incubated with NSPs (10.6 nM HNE; 150 nM Pr3; 140 nM CatG) for 10 min at 30°C for HNE and 37°C for CatG and Pr3. Following incubation, 50 µL of the appropriate chromogenic substrate (2 mM *N*-succinyl-Ala-Ala-Pro-Phe-*p*-nitroanilide and 2 mM *N*-methoxysuccinyl-Ala-Ala-Pro-Val-*p*-nitroanilide) was dispensed to each well of a 96-well plate to reach a final volume of 160 µL. Release of *p*-nitroaniline was monitored by measuring absorbance at 405 nm using a SynergyTM 2 microplate reader equipped with an external dispense module (BioTek Insruments, Inc., Winooski, VT). Enzyme activity was determined by calculating the initial rate of each progression curve in the linear region and was expressed as a percentage of the initial rate of the uninhibited enzyme. Data were analyzed in PrismTM 6 (GraphPad Software, Inc., La Jolla, CA) using nonlinear regression cure fit to determine the half-maximal inhibitory concentration (IC_{50}) values of each compound. The incubation medium used throughout the experiment was 50 mM Tris buffer, pH 7.4, containing 150 mM NaCl and 0.1 mg/mL bovine serum albumin.

Enzyme kinetics study

Initial velocity studies were performed by maintaining the inhibitor concentration at 0, 0.5[IC_{50}], [IC_{50}], 2[IC_{50}] and 4[IC_{50}] and varying the CatG-specific substrate concentration (0.315–2 mM *N*-succinyl-Ala-Ala-Pro-Phe-*p*-nitroanilide). The inhibitors, at the various concentrations, were incubated with CatG (140 nM) for 10 min at 37°C in assay buffer (50 mM Tris buffer, pH 7.4, containing 150 mM NaCl and 0.1 mg/mL bovine serum albumin) after which substrate was rapidly dispensed to each well and the increase in absorbance was measured at 405 nm every 4 s for 1 min. The mechanism of inhibition was determined by fitting the initial velocity at each CatG substrate concentration using Michaelis–Menten kinetics in SigmaPlot (Systat Software, San Jose, CA).

Cell culture

A549 lung epithelial cells were obtained from ATCC (CCL-185). Cells were grown in RPMI-1640 medium supplemented with 10% fetal bovine serum (FBS), 0.1% penicillin–streptomycin and 2 mM Glutamax™ at 37°C and 5% CO_2 atmosphere.

Cell detachment assay

To determine protease-induced cell detachment, A549 cells were seeded at 2×10^4 cells per well in uncoated tissue culture treated 96-well black plates with clear bottom and grown for 18 h in complete growth medium (RPMI-1640 medium supplemented with 10% FBS, 0.1% penicillin–streptomycin and 2 mM Glutamax™). The growth medium was then removed and cells were cultured for 24 h in serum-free medium (RPMI-1640 medium supplemented with 0.1% penicillin–streptomycin). *N*-Arylacyl *O*-sulfonated aminoglycosides at three concentrations (250, 2.5 and 0.025 µM) were incubated on ice for 30 min with enzyme (50 nM HNE, 250 nM CatG or 50 nM Pr3) before addition to cells. Cells were then incubated with compound and enzyme for 24 h after which supernatant was removed and cells stained with Hoechst 33342 nuclear dye. Cells in each well were imaged and counted using Operetta High Content Imaging System and Harmony Analysis Software (PerkinElmer Inc.).

Statistical analysis

Nonparametric data were analyzed by the Mann–Whitney *U*-test using GraphPad Prism 6 (GraphPad Software, La Jolla). A *P*-value of 0.05 or less was considered to be significant. Error bars in all figures indicate means ± SE.

Supplementary data

Supplementary data for this article are available online at http://glycob.oxfordjournals.org/.

Funding

This work was supported by a predoctoral fellowship to A.M.F. from the American Chemical Society Division of Medicinal Chemistry sponsored by Bristol-Myers Squibb and a National Institutes of Health National Institute of General Medical Sciences Training Grant in Pharmacological Sciences (Grant T32GM067795).

Acknowledgements

We thank Dr. David Roman and his research group for providing expertise in performing the cell-based studies. The UIHTS facility at University of Iowa is

acknowledged for service to the project, which is supported by NIH grants #S10 RR029274-01 and #P30 CA86862.

Conflict of interest statement

None declared.

Abbreviations

PMN, polymorphonuclear neutrophils; NSP, neutrophil serine proteases; HNE, human neutrophil elastase; Pr3, proteinase 3; CatG, cathepsin G; PI, protease inhibitor; SLPI, secretory leukocyte protease inhibitor; GAG, glycosaminoglycan.

References

Barnes PJ. 2008. Emerging pharmacotherapies for COPD. *Chest*. 134(6): 1278–1286.

Dias-Baruffi M, Pereira-da-Silva G, Jamur MC, Roque-Barreira MC. 1998. Heparin potentiates in vivo neutrophil migration induced by IL-8. *Glycoconj J*. 15(5):523–526.

Drag M, Salvesen GS. 2010. Emerging principles in protease-based drug discovery. *Nat Rev Drug Discov*. 9(9):690–701.

Fenner AM, Kerns RJ. 2011. Synthesis, separation, and characterization of amphiphilic sulfated oligosaccharides enabled by reversed-phase ion pairing LC and LC-MS methods. *Carbohydr Res*. 346(17):2792–2800.

Fenner AM, Oppegard LM, Hiasa H, Kerns RJ. 2013. Selective inhibition of bacterial and human topoisomerases by arylacyl-sulfonated aminoglycoside derivatives. *ACS Med Chem Lett*. 4(5):470–474.

Fernandez C, Hattan CM, Kerns RJ. 2006. Semi-synthetic heparin derivatives: Chemical modifications of heparin beyond chain length, sulfate substitution pattern and N-sulfo/N-acetyl groups. *Carbohydr Res*. 341(10):1253–1265.

Fleddermann J, Pichert A, Arnhold J. 2012. Interaction of serine proteases from polymorphonuclear leucocytes with the cell surface and heparin. *Inflammation*. 35(1):81–88.

Frommherz KJ, Faller B, Bieth JG. 1991. Heparin strongly decreases the rate of inhibition of neutrophil elastase by alpha 1-proteinase inhibitor. *J Biol Chem*. 266(23):15356–15362.

Gupta VK, Gowda LR. 2008. Alpha-1-proteinase inhibitor is a heparin binding serpin: Molecular interactions with the Lys rich cluster of helix-F domain. *Biochimie*. 90(5):749–761.

Guyot N, Wartelle J, Malleret L, Todorov AA, Devouassoux G, Pacheco Y, Jenne DE, Belaaouaj A. 2014. Unopposed cathepsin G, neutrophil elastase, and proteinase 3 cause severe lung damage and emphysema. *Am J Pathol*. 184(8):2197–2210.

Hahn I, Klaus A, Janze AK, Steinwede K, Ding N, Bohling J, Brumshagen C, Serrano H, Gauthier F, Paton JC, et al. 2011. Cathepsin G and neutrophil elastase play critical and nonredundant roles in lung-protective immunity against Streptococcus pneumoniae in mice. *Infect Immun*. 79(12): 4893–4901.

Hajjar E, Broemstrup T, Kantari C, Witko-Sarsat V, Reuter N. 2010. Structures of human proteinase 3 and neutrophil elastase – so similar yet so different. *FEBS J*. 277(10):2238–2254.

Henry BL, Thakkar JN, Liang A, Desai UR. 2012. Sulfated, low molecular weight lignins inhibit a select group of heparin-binding serine proteases. *Biochem Biophys Res Commun*. 417(1):382–386.

Huang L, Fernandez C, Kerns RJ. 2007. Different protein-binding selectivities for N-acyl heparin derivatives having N-phenylacetyl and heterocycle analogs of N-phenylacetyl substituted in place of N-sulfo groups. *Bioorg Med Chem Lett*. 17(2):419–423.

Huang L, Kerns RJ. 2006. Diversity-oriented chemical modification of heparin: Identification of charge-reduced N-acyl heparin derivatives having increased selectivity for heparin-binding proteins. *Bioorg Med Chem*. 14(7):2300–2313.

Hwang TL, Wang WH, Wang TY, Yu HP, Hsieh PW. 2015. Synthesis and pharmacological characterization of 2-aminobenzaldehyde oxime analogs as dual inhibitors of neutrophil elastase and proteinase 3. *Bioorg Med Chem*. 23(5):1123–1134.

Kessenbrock K, Dau T, Jenne DE. 2011. Tailor-made inflammation: How neutrophil serine proteases modulate the inflammatory response. *J Mol Med (Berl)*. 89(1):23–28.

Korkmaz B, Horwitz MS, Jenne DE, Gauthier F. 2010. Neutrophil elastase, proteinase 3, and cathepsin G as therapeutic targets in human diseases. *Pharmacol Rev*. 62(4):726–759.

Korkmaz B, Moreau T, Gauthier F. 2008. Neutrophil elastase, proteinase 3 and cathepsin G: Physicochemical properties, activity and physiopathological functions. *Biochimie*. 90(2):227–242.

Lu P, Takai K, Weaver VM, Werb Z. 2011. Extracellular matrix degradation and remodeling in development and disease. *Cold Spring Harb Perspect Biol*. 3(12): doi:10.1101/cshperspect.a005058.

Lucas SD, Costa E, Guedes RC, Moreira R. 2013. Targeting COPD: Advances on low-molecular-weight inhibitors of human neutrophil elastase. *Med Res Rev*. 33 (Suppl. 1):E73–E101.

Ohbayashi H. 2002. Neutrophil elastase inhibitors as treatment for COPD. *Expert Opin Investig Drugs*. 11(7):965–980.

Owen CA. 2008. Roles for proteinases in the pathogenesis of chronic obstructive pulmonary disease. *Int J Chron Obstruct Pulmon Dis*. 3(2):253–268.

Owen CA, Campbell EJ. 1999. The cell biology of leukocyte-mediated proteolysis. *J Leukoc Biol*. 65(2):137–150.

Owen CA, Campbell MA, Boukedes SS, Stockley RA, Campbell EJ. 1994. A discrete subpopulation of human monocytes expresses a neutrophil-like proinflammatory (P) phenotype. *Am J Physiol*. 267(6 Pt 1):L775–L785.

Pham CT. 2006. Neutrophil serine proteases: Specific regulators of inflammation. *Nat Rev Immunol*. 6(7):541–550.

Qian Y, Xie H, Tian R, Yu K, Wang R. 2014. Efficacy of low molecular weight heparin in patients with acute exacerbation of chronic obstructive pulmonary disease receiving ventilatory support. *COPD*. 11(2):171–176.

Rao NV, Kennedy TP, Rao G, Ky N, Hoidal JR. 1990. Sulfated polysaccharides prevent human leukocyte elastase-induced acute lung injury and emphysema in hamsters. *Amer Rev Resp Dis*. 142(2):407–412.

Saluja B, Li H, Desai UR, Voelkel NF, Sakagami M. 2014. Sulfated caffeic acid dehydropolymer attenuates elastase and cigarette smoke extract-induced emphysema in rats: Sustained activity and a need of pulmonary delivery. *Lung*. 192(4):481–492.

Saluja B, Thakkar JN, Li H, Desai UR, Sakagami M. 2013. Novel low molecular weight lignins as potential anti-emphysema agents: In vitro triple inhibitory activity against elastase, oxidation and inflammation. *Pulm Pharmacol Ther*. 26(2):296–304.

Sethi S. 2010. Infection as a comorbidity of COPD. *Eur Resp J*. 35(6):1209–1215.

Sissi C, Lucatello L, Naggi A, Torri G, Palumbo M. 2006. Interactions of low-molecular-weight semi-synthetic sulfated heparins with human leukocyte elastase and human Cathepsin G. *Biochem Pharmacol*. 71(3):287–293.

Spencer JL, Stone PJ, Nugent MA. 2006. New insights into the inhibition of human neutrophil elastase by heparin. *Biochemistry*. 45(30):9104–9120.

Turino GM. 2002. The origins of a concept: The protease-antiprotease imbalance hypothesis. *Chest*. 122(3):1058–1060.

Webb LM, Ehrengruber MU, Clark-Lewis I, Baggiolini M, Rot A. 1993. Binding to heparan sulfate or heparin enhances neutrophil responses to interleukin 8. *Proc Natl Acad Sci USA*. 90(15):7158–7162.

Zani ML, Baranger K, Guyot N, Dallet-Choisy S, Moreau T. 2009. Protease inhibitors derived from elafin and SLPI and engineered to have enhanced specificity towards neutrophil serine proteases. *Protein Sci*. 18(3):579–594.

Zani ML, Tanga A, Saidi A, Serrano H, Dallet-Choisy S, Baranger K, Moreau T. 2011. SLPI and trappin-2 as therapeutic agents to target airway serine proteases in inflammatory lung diseases: Current and future directions. *Biochem Soc Trans*. 39(5):1441–1446.